İstanbul Commerce University Journal of Science, 24(47), Spring 2025, 303-317.

İSTANBUL TİCARET ÜNİVERSİTESİ
FEN BİLİMLERİ DERGİSİ

İstanbul Commerce University Journal of Science

http://dergipark.org.tr/ticaretfbd

Research Article / Araştırma Makalesi

DEVELOPMENT OF AN EMBEDDED SYSTEM-BASED COLD CATHODE VACUUM MEASUREMENT SYSTEM FOR (ULTRA HIGH VACUUM) UHV APPLICATIONS

ULTRA YÜKSEK VAKUM UYGULAMALARI İÇİN GÖMÜLÜ SİSTEM TABANLI SOĞUK KATOT VAKUM ÖLÇÜM SİSTEMİNİN GELİŞTİRİLMESİ

Tarık ÜNLER[1]

https://doi.org/10.55071/ticaretfbd.1699770

***Corresponding Author* (*Sorumlu Yazar*)**
tunler@erbakan.edu.tr

***Received* (*Geliş Tarihi*)**	***Revised* (*Revizyon Tarihi*)**	***Accepted* (*Kabul Tarihi*)**
15.05.2025	*22.05.2025*	*03.06.2025*

Abstract

Vacuum measurements are widely utilized in numerous critical applications including defense industries, aerospace technologies, composite material manufacturing, and various industrial processes. The key performance parameters in vacuum systems include measurement range, accuracy, and operational lifetime of the sensing elements. This study presents a comprehensive investigation of an Inverted Magnetron (IMT) cold cathode vacuum measurement sensor, which offers distinct advantages over conventional hot cathode systems, including an extended measurement range, prolonged operational lifetime, and user-friendly operation. The IMT cathode configuration demonstrates superior performance in low-pressure regimes (below 10^{-3} Torr) by optimizing electron trajectories through magnetic field confinement, thereby achieving high ionization efficiency. To optimize sensor performance, a high-stability digital electronic readout system was designed and implemented. Experimental characterization was conducted using a turbo-molecular vacuum pump, with measurement results successfully demonstrating the system's capability to accurately measure vacuum levels down to 9,9 $\times 10^{-8}$ Torr. These findings validate the IMT cathode design's exceptional stability and wide dynamic range in ultra-high vacuum applications. The developed flexible electronic system enables high-precision digital measurement and control of vacuum systems. This research contributes to the development of an economical, long-lifetime vacuum measurement system capable of stable operation at low-pressure regimes, based on IMT cathode technology.

Keywords: Vacuum measurement, cold cathode ionization sensor, electronic design, low pressure measurement.

Öz

Vakum ölçümleri, savunma sanayisi, uzay teknolojileri, kompozit malzeme üretimi ve endüstriyel uygulamalar gibi birçok kritik alanda yaygın olarak kullanılmaktadır. Vakum sistemlerinde performansı belirleyen temel parametreler arasında ölçüm aralığının genişliği, ölçüm hassasiyeti ve sensör kullanım ömrü yer almaktadır. Bu çalışmada, sıcak katot sistemlere kıyasla daha geniş ölçüm aralığı, uzun kullanım ömrü ve kullanım kolaylığı sunan Inverted Magnetron (IMT) soğuk katot vakum ölçüm sensörü detaylı bir şekilde incelenmiştir. IMT katot yapısı, düşük basınçlarda (10^{-3} Torr altı) manyetik alan etkisiyle elektron hareketini optimize ederek yüksek iyonizasyon verimliliği sağlamasıyla öne çıkmaktadır. Sensörün performansını optimize etmek amacıyla, dijital okuma yapabilen yüksek kararlılığa sahip bir elektronik sistem tasarlanmış ve turbo moleküler vakum pompası ile deneysel karakterizasyon çalışmaları gerçekleştirilmiştir. Yapılan deneysel çalışmalar sonucunda, IMT katot soğuk katot sensör ile 9,9 $\times 10^{-8}$ Torr seviyesine kadar olan vakum değerleri başarıyla ölçülmüştür. Bu sonuçlar, IMT katot tasarımının düşük basınç uygulamalarında sunduğu stabilite ve geniş dinamik aralığın bir göstergesidir. Tasarlanan esnek elektronik sistem sayesinde, vakum sistemlerinde yüksek hassasiyetle dijital ölçüm ve kontrol imkânı sağlanmıştır. Bu çalışma, IMT katot teknolojisini temel alan ekonomik, uzun ömürlü ve düşük basınç seviyelerinde kararlı ölçüm yapabilen bir vakum ölçüm sisteminin geliştirilmesine katkı sunmaktadır.

Anahtar Kelimeler: Vakum ölçümü, soğuk katot iyonizasyon sensörü, elektronik tasarım, düşük basınç ölçümü.

[1] Necmettin Erbakan University, Faculty of Aviation and Space Sciences, Department of Avionics, Konya, Türkiye. tunler@erbakan.edu.tr.

1. INTRODUCTION

Vacuum measurement technology plays a vital role across a wide range of industrial and scientific fields, serving as an essential tool for achieving and maintaining controlled environments required for specific processes. In the semiconductor industry, vacuum systems are indispensable for procedures such as thin-film deposition and etching, where precise pressure control is critical to ensuring the desired quality of semiconductor components (Li et al., 2021). Similarly, in the food and beverage industry, vacuum technology is employed to extend product shelf life and preserve quality during packaging and processing, with accurate pressure measurement being crucial for these applications (Hubbard et al., 2021). Vacuum measurement also plays a critical role in space research, where vacuum chambers are used to simulate extraterrestrial conditions, thereby ensuring the reliability of experiments and the performance of materials intended for outer space applications (Li et al., 2021). Moreover, in space programs, vacuum measurement technology is essential for enhancing the performance of satellites and spacecraft (Chen et al., 2023). In the pharmaceutical industry, vacuum environments are essential for sterile manufacturing processes, where maintaining precise pressure levels is vital for production control and operational safety (Hubbard et al., 2021). Furthermore, vacuum technology supports material characterization studies, allowing researchers to investigate the physical and chemical properties of materials under controlled conditions, thereby improving the accuracy of experimental outcomes (Fu, 2024; Zhou et al., 2014). Recent advancements such as cold atom vacuum metrology have significantly enhanced measurement accuracy, enabling highly sensitive pressure readings in the range of 10^{-4} to 10^{-10} Pa (Fu, 2024). These developments reflect the continuous evolution of vacuum measurement technologies to meet growing demands for precision and reliability in various applications. This study reviews the utilization of vacuum measurement technologies in key industrial and scientific domains and analyzes the measurement methodologies employed, highlighting their contributions to technological and process advancements. The effectiveness of vacuum systems largely depends on the precision and reliability of the measurement methods used. Among these, Pirani gauges, which operate based on thermal conductivity principles, provide accurate readings in low to medium vacuum ranges (Wei et al., 2019; Song, 2024). Thermocouple gauges are often preferred in high-temperature environments due to their robust performance under extreme conditions (Wei et al., 2019). For ultra-high vacuum (UHV) conditions, ionization gauges offer exceptional precision by utilizing gas molecule ionization (Fu, 2024; Li et al., 2021). Capacitance manometers, which determine pressure through changes in the capacitance of a sensor, are favored for their accuracy in low-pressure scenarios (Shirhatti et al., 2020; Wei et al., 2019). In recent years, novel techniques such as cold atom technology have been introduced for vacuum measurement, providing the capability for highly sensitive measurements in extremely low-pressure environments (Li et al., 2021). Additionally, graphene-based sensors have gained attention for their high sensitivity and rapid response times (Shirhatti et al., 2020; Zhu et al., 2019). Advanced technologies such as microelectromechanical systems (MEMS) offer compact and highly sensitive solutions for vacuum measurement applications (Song, 2024; Takashima & Kimura, 2008). Pirani gauges function based on the principle of wire heating, where the temperature of the wire changes according to the pressure of the surrounding gas, allowing for accurate pressure measurements in low-pressure ranges (Song, 2024; Takashima & Kimura, 2008). MEMS-based Pirani

sensors are particularly notable for their smaller size and enhanced sensitivity (Chen et al., 2023; Xiao et al., 2010). Cold cathode gauges operate on the principle of gas ionization through electrical current and are preferred in high vacuum applications for their high measurement accuracy (Fu, 2024; Takashima & Kimura, 2008). Hot cathode gauges measure ions generated by electron interactions with gas molecules, offering high precision but requiring high operating temperatures and currents, which makes the system more complex (Fu, 2024; Li et al., 2021). Capacitance sensors are widely used in industry for pressure, flow, and level measurements, offering advantages such as high accuracy and low power consumption (Shirhatti et al., 2019; Lee et al., 2006). They are also effectively utilized in vacuum measurement applications (Teotia, 2023).
In vacuum measurement, both cold and hot cathode technologies present distinct advantages and disadvantages that are critical for various scientific and engineering applications. Understanding these differences is important for selecting the appropriate technology based on specific measurement requirements. Cold cathode gauges, especially those incorporating materials such as carbon nanotubes (CNTs), offer several advantages over hot cathode devices. Their ability to emit electrons without preheating results in lower power consumption and operational simplicity. These features enable fast response times and miniaturization, making them suitable for field emission displays (FEDs) and other microelectronic devices (Shao et al., 2018; Chen et al., 2021; Chen, 2023). Moreover, due to their lower sensitivity to environmental conditions, cold cathodes exhibit enhanced stability and reliability across various operating environments (Shimawaki et al., 2010; Yamaguchi et al., 2003). They are capable of achieving high brightness and uniform electron emission across large areas, making them especially advantageous for applications requiring consistent performance over wide surfaces (Shimawaki et al., 2010; Yamaguchi et al., 2003). The chemical inertness of materials such as graphene and CNTs reduces vulnerability to performance degradation from residual gas adsorption, thereby contributing to improved long-term stability (Shao et al., 2018; Zhang et al., 2021). Additionally, the “cold” nature of their operation minimizes outgassing, offering significant benefits for UHV and extreme high vacuum (XHV) measurements (Shimawaki et al., 2010; Yamaguchi et al., 2003). However, cold cathode gauges also present certain limitations. A notable drawback is their sensitivity to outgassing, which can lead to performance degradation over time. Research indicates that outgassing increases with emission current density, potentially compromising the accuracy of vacuum measurements (Yamaguchi et al., 2003). Although cold cathodes are highly effective under UHV conditions, they may not perform as well as hot cathodes in low vacuum ranges (Cui et al., 2011; Yang et al., 2008). Hot cathode devices, such as thermionic emission ionization gauges, represent a well-established technology for measuring pressures from low to ultra-high vacuum. They offer high measurement precision, particularly in pressures below 10^{-1} Pa, due to their robust electron emission capabilities (Wang & Yu, 2015). The thermionic emission process allows hot cathodes to generate a substantial number of electrons, which enhances sensitivity under low-pressure conditions. The long-standing use and well-developed infrastructure around hot cathodes make them a reliable choice for many traditional applications (Wang & Yu, 2015). Their effectiveness across a broader vacuum range, particularly in low vacuum environments, further reinforces their reliability (Wang & Yu, 2015; Krishnan & Cahay, 2003). Nonetheless, hot cathodes also exhibit some disadvantages. Their high-temperature requirements lead to increased power consumption and longer warm-up periods, posing limitations for applications requiring rapid response times (Shao et al., 2018). Thermal operation may result in

filament degradation and contamination due to outgassing, which can compromise measurement accuracy over time (Wang & Yu, 2015). Thermal noise and operational instability may also present concerns, especially in precision measurement contexts (Wang & Yu, 2015).

In conclusion, the choice between cold and hot cathode vacuum measurement technologies depends on the specific application requirements, including desired pressure range, response time, power consumption, and environmental stability. While cold cathodes offer advantages in terms of efficiency and miniaturization, hot cathodes provide robustness and reliability for low-pressure measurements. In this study, an Inverted Magnetron (IMT) cold cathode vacuum measurement sensor was selected due to its superior performance characteristics, such as extended operational lifetime, wide measurement range, and cost-effectiveness compared to conventional hot cathode systems. Leveraging the advantages of IMT technology—particularly its high ionization efficiency in low-pressure regimes a vacuum measurement system capable of operating down to 10^{-8} Torr was developed. The sensor features an analog output, and a high-stability digital readout circuit was specifically designed and implemented to enhance measurement precision. Experimental measurements were carried out using a turbo-molecular pump supported by an auxiliary pump, confirming the system's effectiveness in ultra-high vacuum applications. The results validate the IMT cathode's suitability for long-term, accurate measurements in advanced vacuum

2. METERIAL AND METHOD

In this study, a cold cathode vacuum sensor was integrated with a custom-designed electronic circuit to enable accurate measurement and digital display of vacuum levels down to 10^{-10} Torr. To generate the required vacuum environment, the experimental setup was constructed using one Edwards backing pump and one Pfeiffer turbo molecular pump, connected via sealed clamps, gaskets, and flexible metal hoses to ensure vacuum-tight integrity. The developed system allowed real-time monitoring of ultra-high vacuum conditions, demonstrating the sensor's capability to operate reliably within extremely low-pressure ranges. This setup validates both the effectiveness of the cold cathode sensor and the stability of the electronic readout system for high precision vacuum applications.

2.1. System Components and Instrumentation

In this study, the Inverted Magnetron Transducer (IMT) used is the MKS 903, a compact cold cathode vacuum sensor equipped with an integrated electronic module. This sensor operates based on cold cathode ionization principles to measure vacuum pressure. It is available with four standard vacuum interface options: KF 25, KF 40, 2¾" CF (rotatable), and 1" tube; the KF 25 interface was selected for the present study. The primary function of the IMT sensor is pressure measurement, specifically designed for applications requiring measurements in the pressure range of 3×10^{-10} to 5×10^{-3} Torr. It features fast response time and a wide dynamic measurement range. Pressure readings are obtained through a linear voltage output ranging from 1,5 to 8,7 V (DC). Compared to hot cathode sensors, cold cathode sensors such as the IMT offer several advantages: absence of a consumable filament, immunity to convective air currents, resistance to vibration-induced damage, elimination of x-ray limit issues at low pressures, no need for emission current adjustment, and reusability of the sensor tube after cleaning. The inverted magnetron geometry used in the IMT enhances measurement repeatability by providing a more consistent conductivity-pressure curve and ensures stable discharge operation without the risk of extinction at low pressures. The sensor is factory-calibrated for air/nitrogen. When used with other gases, the output corresponds to an equivalent nitrogen pressure; thus, correction factors or additional calibration are required for accurate measurement. This gas dependency also makes the sensor suitable for leak detection applications. The IMT sensor is designed for maintenance-free operation under normal conditions. However, contamination of the sensor tube may result in unstable or inaccurate readings. Prolonged operation at pressures above 10^{-3} Torr can accelerate contamination. Nevertheless, the sensor can be restored by cleaning the internal components and reused. Figures 1(a) and 1(b) show the sensor unit and the corresponding pin diagram, respectively.

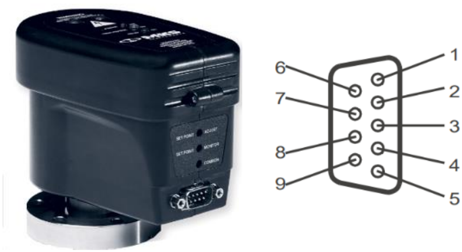

Standard		Alternate	
1	Relay - NO	1	HV enable
2	Relay - NC	2	- VIN
3	+ VIN	3	Analog Output (+)
4	- VIN	4	+ VIN
5	Analog Output (+)	5	no conn
6	Relay - Common	6	no conn
7	Relay - Disable	7	Analog Output (-)
8	Analog Output (-)	8	no conn
9	HV enable	9	Status

(a) (b)

Figure 1. MKS 903 sensor (a) and Pinout (b)

As illustrated in Figure 1(b), pins 2 and 3 of the sensor were utilized to provide the required power supply. According to the sensor's technical documentation, the operating voltage range for the power supply is specified as 14–30 V (DC), with a maximum power consumption of 3 W. For the analog output signal, pins 3 and 7 were used. Additionally, pin 1 was employed to enable the High Voltage (HV) supply of the sensor, ensuring proper measurement initiation. An RS232 connector was employed to interface both the power supply and analog signal connections. To process the analog voltage signal from the sensor, an Arduino Nano microcontroller was used. The measured pressure values were displayed in real time using a 2-line, 16-character alphanumeric display unit. This configuration allowed for a compact, low-cost, and effective monitoring solution for vacuum measurements. The Arduino Nano and display unit utilized in the system are shown in Figure 2.

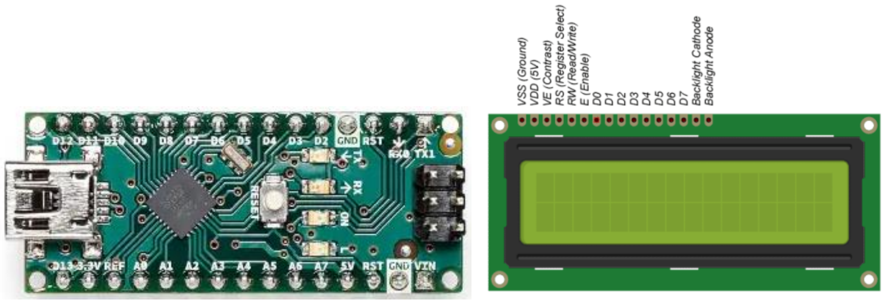

(a) (b)

Figure 2. Arduino Nano (a) 2-line 16-character Display (b)

Since the sensor provides an analog voltage output in the range of 0–10 V, it was necessary to adapt this voltage level to be compatible with the input range of the Arduino Nano, which operates at a maximum input voltage of 5 V on its analog pins. To achieve this, a simple resistive voltage divider circuit was implemented, effectively scaling down the sensor output to a level suitable for safe and accurate analog-to-digital conversion by the microcontroller.

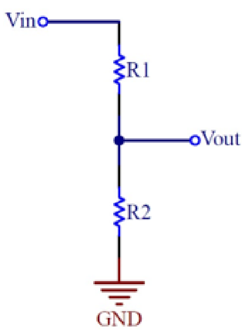

Figure 3. Voltage Divider Circuit

Figure 3 illustrates the voltage divider circuit used in the system for voltage matching. In this configuration, V_{in} represents the input voltage, which is the sensor's output voltage. The V_{out} is the voltage that is fed to the analog input pin of the Arduino Nano, which will be used for the pressure measurement. The output voltage V_{out} can be calculated as shown in Equation 1.

$$V_{out} = \frac{R_2}{R_1+R_2} V_{in} \tag{1}$$

When the values of R1 and R2 are calculated using the equation, it is observed that in order to reduce a 10V input to 5V, the resistance values of R1 and R2 must be equal. Accordingly, considering the current value, the resistors are chosen to be 1kΩ. In order to achieve low vacuum levels (down to 10^{-8} Torr), a Pfeiffer Vacuum TMH 071P turbo-molecular vacuum pump and an Edwards back pump were used in the system. The Edwards back pump has a vacuum capacity of 10^{-4} Torr, and when used in conjunction with the Pfeiffer vacuum pump, it can achieve vacuum levels down to 10^{-8} Torr. The vacuum pumps used in the system are shown in Figure 4.

Figure 4. Edwards Back Pump (a) Pfeiffer TMH 071P Vacuum Pump (b)

All connections in the system have been made using KF25 and KF10 fittings. Additionally, to prevent leakage during measurements, the system termination has been achieved with a gasket and a termination plug, ensuring a leak-free setup. For the power supply, a 220V AC to 24V DC, 4A SMSP (Switching Mode Power Supply) has been used to power the sensor, the Pfeiffer vacuum pump, and the electronic systems.

Figure 5. 24V 4A AC/DC Switching Mode Power Supply (SMSP)

Figure 5 illustrates the use of the SMPS converter in the system. This converter was selected due to its current limiting capabilities, which are crucial for protecting the pump motor in case of any malfunctions in the vacuum pump. The current limitation feature ensures that the pump motor is safeguarded against potential damage. For the electronic systems, the 24V output from the power supply is regulated to 5V using a voltage regulator, making the system compatible with the required specifications.

2.2. Measurement System and Experimental Setup

The most critical components of the measurement system are the MKS903 sensor and the microcontroller system responsible for reading the data from the sensor. The sensor provides an analog voltage output in the range of 0–10 V for pressure values between 3×10^{-10} Torr and 5×10^{-3} Torr. However, this voltage varies in direct proportion to the pressure. The relationship between pressure and voltage is logarithmic in nature. In order to convert these values into a more understandable form, it is necessary to linearize them numerically through the embedded system.

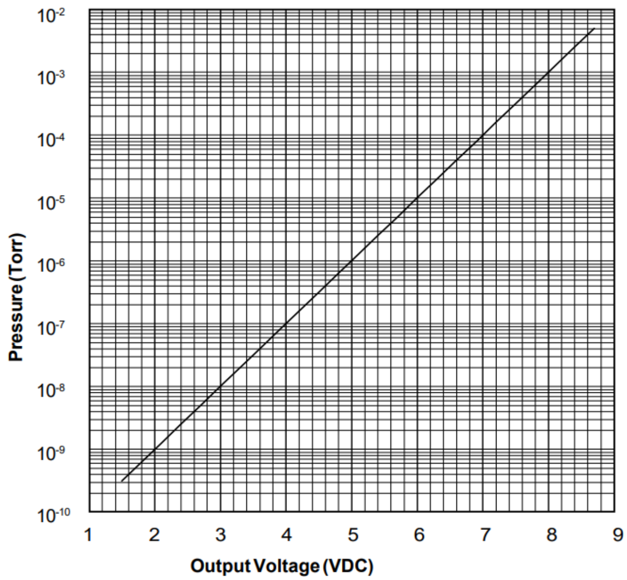

Figure 6. Relationship between Pressure and Output Voltage

Upon examining the graph in Figure 6, it is evident that there is no linear relationship between pressure and voltage. Therefore, an additional calculation is required for the conversion. The MKS 903 catalog suggests using the equation provided in Equation 2 for pressure measurement calculations, specifically for air or nitrogen.

$$P_{indicated} = 10^{(V-K)} \quad (2)$$

In Equation 2, P indicates the pressure for air and nitrogen in Torr, mbar, microns, or Pascal (depending on K), and V represents the voltage for $1,5 < V < 8,7$. The constant K takes the following values: 11000 for Torr, 10875 for mbar, 8000 for microns, and 8875 for Pascal. The calculation process was performed using a software application, facilitated by the microcontroller. Additionally, since the analog input level of the microcontroller is 5V, a voltage converter was used to adjust the voltage range to 0-5V. Measurements were calculated in Torr, using the commonly employed constant K=11000 for vacuum systems, and the results were displayed on the screen.

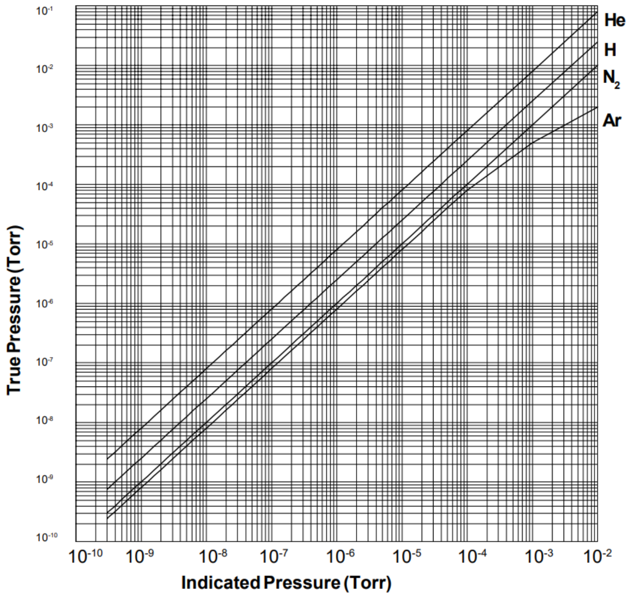

Figure 7. Relationship Between $P_{indicated}$ and True Pressure for Different Gases

In Figure 7, the relationship between the indicated pressure ($P_{indicated}$) and the actual pressure values in Torr for different gases is presented. The graph provides values for four gases commonly used in the system: hydrogen, helium, nitrogen, and argon.

Table 1. Gas Correction Factors for Series 903 (IMT) Cold Cathode Ionization Gauge

Gas	Correction Factor (True Pressure/İndicated Pressure)	Applicable Pressure Range (Torr)
Hydrogen (H_2)	2,5	3×10^{-10} to 5×10^{-3}
Helium (He)	8	3×10^{-10} to 5×10^{-3}
Argon (Ar)	0,8	Below 1×10^{-4}
Argon (Ar)	0,5	Around 1×10^{-3}
Argon (Ar)	0,2	Around 1×10^{-2}

For gases other than air and nitrogen, the correction factors provided in Table 1 should be applied. The following equation, as given in the sensor catalog, must be used for vacuum pressure measurements of these gases.

$$P_{Gas} = P_{indicated} \times \text{Correction Factor} \tag{3}$$

In the equation, $P_{indicated}$ represents the value calculated for air. The pressure value for the gas to be measured can be obtained by multiplying this value by the correction factor of the specific gas, as provided in Table 2. For argon (Ar), as shown in Figure 6, the variation in pressure is more erratic compared to other gases in certain regions, which means that the correction factor will vary depending on the measurement range. The schematic of the experimental setup is shown in Figure 8.

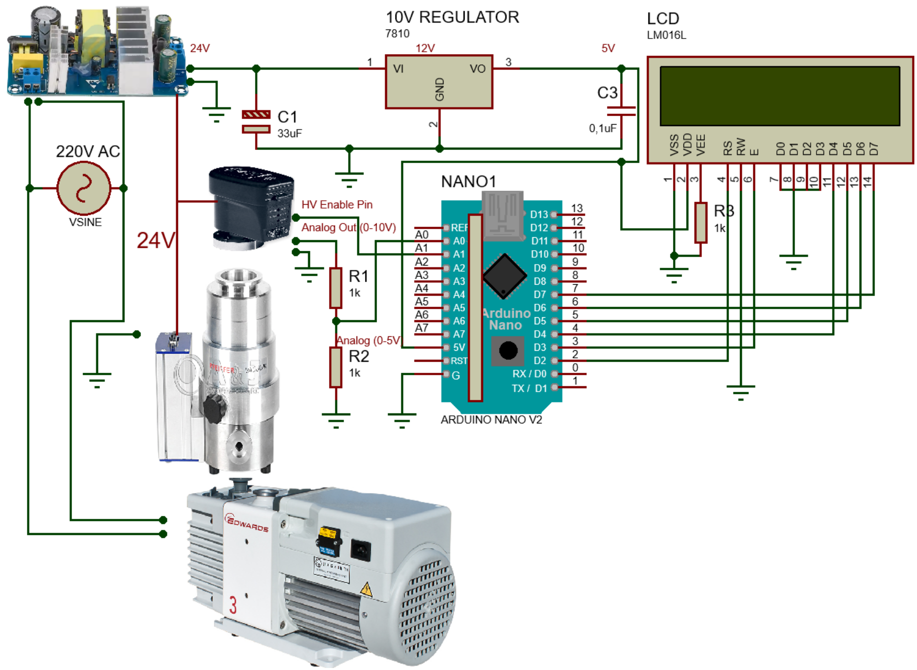

Figure 8. Measurement System and Experimental Setup Diagram

The experimental setup consists of a MKS 903 cold cathode sensor, an Arduino Uno embedded system for reading analog data, an LCD screen for displaying pressure values, a voltage divider for adapting the sensor data to the embedded system's conversion voltage (from 0-10V to 0-5V), and a 24V DC power supply. Additionally, two voltage regulators are employed for the electronic board. To prevent excessive heat generation caused by the large voltage drop, the 24V input is first stepped down to 10V using a 7810 linear regulator before being further reduced to 5V by the microcontroller board's onboard voltage regulator, ensuring efficient and stable power conversion. This approach enhances both the system's performance and safety. Furthermore, the regulator serves as a filter, preventing parasitic signals from the power supply and isolating the pump system from any noise in the voltage source. The A0 pin is configured as an analog input to read the analog data received from the sensor. The A1 pin is set as a digital output to enable the sensor's High Voltage (HV) pin and initiate the measurement process. For the display interface, the D2 and D3 pins are connected to the RS (Register Select) and EN (Enable) control lines, respectively, while the D4, D5, D6, and D7 pins are assigned as the data lines to establish communication with the display module, thereby finalizing the circuit design. All connections within the system are mounted on the PCB using connectors, making the system modular. For the vacuum measurement, the Edwards back pump is connected to the Pfeiffer vacuum pump using a flexible metal pipe, with a KF25-KF10 adapter employed at the Pfeiffer end. The connection is made with flexible pipes and seals. In the experimental setup, the sensor is connected to the Pfeiffer vacuum pump via a T-adapter with a three-way KF25 connection, along with a KF25 connection fitting and KF25 seal. The third port of the T-adapter is terminated with a KF25 cap and seal, ensuring the system's vacuum tightness. This setup ensures that the system is ready for accurate vacuum measurement.

2.3. Experimental Setup and Vacuum Measurement Results

Within the scope of this study, vacuum measurements were conducted utilizing an experimental apparatus incorporating an integrated sensor and electronic circuitry. The measurement accuracy was validated through comparative analysis with an MKS903 reference vacuum gauge, which serves as an industry standard measurement device. Figure 9 provides a comprehensive illustration of the specifically designed experimental configuration implemented for vacuum measurement purposes.

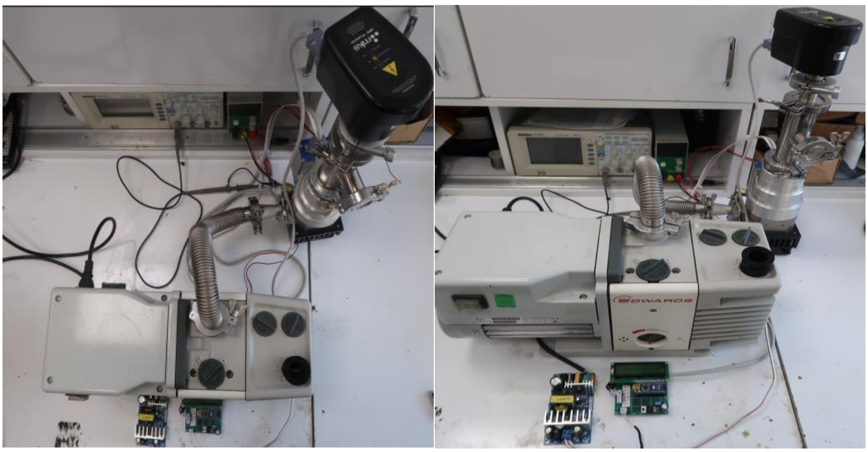

Figure 9. Experimental Setup for Vacuum Measurement

During testing, while measurement errors were observed at low vacuum levels, it was determined that the system achieved stable measurements and consistently displayed values on the screen as vacuum levels increased. This behavior is consistent with the manufacturer's specifications and, therefore, expected. Considering the reference MKS903 device's measurement capability in the range of 3×10^{-10} Torr to 5×10^{-3} Torr, these deviations in the low vacuum region were considered within acceptable limits. Notably, below 5×10^{-3} Torr, the system demonstrated significantly improved measurement stability and began reading true vacuum values with high accuracy.

Figure 10. Measurement Results of Various Vacuum Levels Using the Experimental Setup

The experimental setup presented in Figure 10, through its high voltage (HV) control strategy, protected the sensor from adverse effects in low vacuum regions and successfully performed extremely stable and reliable measurements in the $9{,}9\times10^{-4}$ Torr to $9{,}9\times10^{-8}$ Torr range. These successful results, achieved through hardware optimization and integrated measurement algorithms, demonstrate that the system provides an advanced solution for both academic research and industrial applications.

3. CONCLUSION

In this study, an embedded system-based cold cathode vacuum measurement sensor employing Inverted Magnetron (IMT) cathode technology was designed and experimentally characterized. The system demonstrated stable measurement performance, particularly in the ultra-high vacuum (UHV) regime below 10^{-4} Torr, with comparative testing against the reference MKS903 sensor confirming accurate measurements down to $9{,}9\times10^{-8}$ Torr. The optimization of electron trajectories through magnetic field confinement enabled the sensor to achieve high ionization efficiency at low pressures. Furthermore, the implemented digital electronic readout system effectively compensated for the sensor's non-linear output characteristics through mathematical modeling, thereby enhancing the precision of real-time measurements.

The key advantages of the developed system can be summarized as follows:

1. Extended Measurement Range: The system offers a broader dynamic range compared to conventional hot cathode systems, particularly in UHV conditions below 10^{-3} Torr.
2. Extended Operational Lifetime: The cold cathode configuration eliminates filament consumption, significantly reducing maintenance requirements and ensuring industrial operational continuity.
3. Energy Efficiency: With a maximum power consumption of 3 W, the system contributes to environmental sustainability while maintaining high performance.
4. Modular Design: The microcontroller-based electronic interface and KF25 vacuum connections enhance the system's adaptability to diverse applications.

In conclusion, the developed system presents an economical and reliable alternative for high-precision applications in defense industries, aerospace technologies, and semiconductor manufacturing. The advantages offered by IMT cathode technology pave the way for next-generation cold cathode applications in vacuum measurement systems, demonstrating significant potential for both academic research and industrial implementation.

Conflict of Interest Statement

The authors declare that they have no competing interests related to the content of this manuscript.

Ethical and Informed Consent for Data Used

Ethical approval and informed consent for data use were not required for this research, as the study did not involve human subjects, personal data, or sensitive information. The data utilized were obtained from publicly available and anonymized sources, and all aspects of the research adhered to ethical standards and legal requirements.

REFERENCES

Arpornthip, T., Sackett, C. A., & Hughes, K. J. (2012). Vacuum-pressure measurement using a magneto-optical trap. Physical Review A—Atomic, Molecular, and Optical Physics, 85(3), 033420 doi:10.1103/physreva.85.033420.

Calcatelli, A. (2013). The development of vacuum measurements down to extremely high vacuum–XHV. Measurement, 46(2), 1029-1039 doi:10.1016/j.measurement.2012.08.018.

Chen, S., Feng, L., Guo, S., Ji, Y., Zeng, S., Peng, X., ... & Wang, S. (2023). A composite-type MEMS Pirani gauge for wide range and high accuracy. Sensors, 23(3), 1276 doi:10.3390/s23031276.

Cui, Y., Zhang, X., Lei, W., Wang, J., Di, Y., Yang, X., & Chen, J. (2012). Effect of outgassing on the field emission property of tetrapod ZnO. physica status solidi c, 9(1), 44-47 doi:10.1002/pssc.201084163.

Fu, Z., Huang, X., Li, J., Yang, S., & Zheng, J. (2024, March). Review of cold atom quantum-based vacuum metrology. In Advanced Fiber Laser Conference (AFL2023) (Vol. 13104, pp. 56-65). SPIE doi:10.1117/12.3016054.

Grzebyk, T., Górecka-Drzazga, A., Dziuban, J. A., Maamari, K., An, S., Dankovic, T., ... & Busta, H. (2015). Integration of a MEMS-type vacuum pump with a MEMS-type Pirani pressure gauge. Journal of Vacuum Science & Technology B, 33(3) doi:10.1116/1.4903448.

Guangci, Z., Stephen, R., Tao, W., & Nay, Y. (2014). Fuel Heat of Vaporization Values Measured with Vacuum Thermogravimetric Analysis Method.

Hubbard, B. R., Putman, L. I., Techtmann, S., & Pearce, J. M. (2021). Open source vacuum oven design for low-temperature drying: performance evaluation for recycled PET and biomass. Journal of Manufacturing and Materials Processing, 5(2), 52 doi:10.3390/jmmp5020052.

Jousten, K., Boineau, F., Bundaleski, N., Illgen, C., Setina, J., Teodoro, O. M., ... & Wüest, M. (2020). A review on hot cathode ionisation gauges with focus on a suitable design for measurement accuracy and stability. Vacuum, 179, 109545 doi:10.1016/j.vacuum.2020.109545.

Krishnan, R., & Cahay, M. (2003). Transition from sub-Poissonian to super-Poissonian shot noise in planar cold cathodes. Journal of Vacuum Science & Technology B: Microelectronics and Nanometer Structures Processing, Measurement, and Phenomena, 21(4), 1278-1285 doi:10.1116/1.1575251.

Lee, K. R., Kim, K., Park, H. D., Kim, Y. K., Choi, S. W., & Choi, W. B. (2006, April). Fabrication of capacitive absolute pressure sensor using Si-Au eutectic bonding in SOI wafer. In Journal of Physics: Conference Series (Vol. 34, No. 1, p. 393). IOP Publishing doi:10.1088/1742-6596/34/1/064.

Li, D., Wang, Y., Zhang, H., Xi, Z., & Li, G. (2021). Applications of vacuum measurement technology in china’s space programs. Space: Science & Technology doi:10.34133/2021/7592858.

Shirhatti, V., Kedambaimoole, V., Nuthalapati, S., Neella, N., Nayak, M. M., & Rajanna, K. (2019). High-range noise immune supersensitive graphene-electrolyte capacitive strain sensor for biomedical applications. Nanotechnology, 30(47), 475502 doi:10.1109/jmems.2024.3367380.

Song, X., Huang, L., Lin, Y., Hong, L., & Xu, W. (2024). Surface Micromachined CMOS-MEMS Pirani Vacuum Gauge With Stacked Temperature Sensor. Journal of Microelectromechanical Systems doi:10.1109/jmems.2024.3367380.

Sparks, D., Queen, G., Weston, R., Woodward, G., Putty, M., Jordan, L., ... & Jayakar, K. (2001). Wafer-to-wafer bonding of nonplanarized MEMS surfaces using solder. Journal of Micromechanics and Microengineering, 11(6), 630 doi:10.1088/0960-1317/11/6/303.

Takashima, N., & Kimura, M. (2008). Investigation on the Thin Film Pirani Vacuum Sensor Using A Constant Voltage Drive-Mode Diode-Heater. IEEJ Transactions on Sensors and Micromachines, 128(5), 209-213 doi:10.1541/ieejsmas.128.209.

Wang, J. Q., & Yu, J. (2015). Fabrication process and electro-thermal modeling for the cathode of the cmos-compatible hot-filament vacuum gauge. Key Engineering Materials, 645, 836-840 doi:10.4028/www.scientific.net/kem.645-646.836.

Wei, D., Fu, J., Liu, R., Hou, Y., Liu, C., Wang, W., & Chen, D. (2019). Highly sensitive diode-based micro-Pirani vacuum sensor with low power consumption. Sensors, 19(1), 188 doi:10.3390/s19010188.

Yang, Y., Qian, L., Tang, J., Liu, L., & Fan, S. (2008). A low-vacuum ionization gauge with HfC-modified carbon nanotube field emitters. Applied Physics Letters, 92(15) doi:10.1063/1.2909467.

Yuan, X., Zhu, W., Zhang, Y., Xu, N., Yan, Y., Wu, J., ... & Deng, S. (2016). A fully-sealed carbon-nanotube cold-cathode terahertz gyrotron. Scientific Reports, 6(1), 32936 doi:10.1038/srep32936.

Zhang, J., Li, D., Zhao, Y., Cheng, Y., & Dong, C. (2016). Wide-range vacuum measurements from MWNT field emitters grown directly on stainless steel substrates. Nanoscale Research Letters, 11, 1-7 doi:10.1186/s11671-016-1956-6.

Zhang, J., Wei, J., Li, D., Zhang, H., Wang, Y., & Zhang, X. (2021). A Cylindrical Triode Ultrahigh Vacuum Ionization Gauge with a Carbon Nanotube Cathode. Nanomaterials, 11(7), 1636 doi:10.3390/nano11071636.

Zhou, G., Roby, S., Wei, T., & Yee, N. (2014). Fuel heat of vaporization values measured with vacuum thermogravimetric analysis method. Energy & fuels, 28(5), 3138-3142 doi:10.1021/ef402491p.

Zhu, Y., Cai, H., Ding, H., Pan, N., & Wang, X. (2019). Fabrication of low-cost and highly sensitive graphene-based pressure sensors by direct laser scribing polydimethylsiloxane. ACS applied materials & interfaces, 11(6), 6195-6200 doi:10.1021/acsami.8b17085